RESTRICTED INVESTIGATION REPORT 1692R

CSIRO

INSTITUTE OF ENERGY AND EARTH RESOURCES

DIVISION OF MINERAL PHYSICS AND MINERALOGY

MAGNETIC PROPERTIES OF GOLDEN MILE DOLERITE SAMPLES

D.A. CLARK

P.O. Box 136
North Ryde, NSW
Australia 2113

MAY, 1987

CSIRO

Division of Mineral Physics and Mineralogy
Delhi Road, North Ryde, NSW, Australia

A Division of the Institute of Energy and Earth Resources

CHIEF
Dr B. J. J. Embleton

PO Box 136, North Ryde, NSW, Australia 2113
Telephone (02) 887 8666
Telex AA25817
Facsimile (02) 887 8909

POLICY ON RESTRICTED INVESTIGATION REPORTS

Restricted Investigation Reports issued by this Division deal with projects where CSIRO has been granted privileged access to research material. In return for this access, they provide recipients with an opportunity to take advantage of results obtained on their samples or problems. Initially, circulation of Restricted Investigation Reports is strictly controlled, and we treat them as confidential documents at this stage. They should not be quoted publicly, but may be referred to as a "personal communication" from the author(s) if my approval is sought and given beforehand.

The results embodied in a Restricted Investigation Report may eventually form part of a more widely circulated CSIRO publication. Agreements with sponsors or companies generally specify that drafts will be first submitted for their approval, to ensure that proprietary information of a confidential nature is not inadvertently included.

After a certain period of time, the confidentiality of particular Restricted Investigation Reports will no longer be an important issue. It may then be appropriate for CSIRO to announce the titles of such reports, and to allow inspection and copying by other persons. This procedure would disseminate information about CSIRO research more widely to Industry. However, it will not be applicable to all Restricted Investigation Reports. Proprietary interests of various kinds may require an extended period of confidentiality. Premature release of Restricted Investigation Reports arising from continuing collaborative projects (especially AMIRA projects) may also be undesirable, and a separate policy exists in such cases.

You are invited to express an opinion about the security status of the enclosed Restricted Investigation Report. Unless I hear to the contrary, I will assume that in eighteen months time I have your permission to place this Restricted Investigation Report on open file, when it will be generally available to interested persons for reading, making notes, or photocopying, as desired.

B.J.J. Embleton
CHIEF OF DIVISION

CONTENTS

LIST OF TABLES

LIST OF FIGURES

DISTRIBUTION LIST

	Copy No.
CSIRO Division of Mineral Physics	
D. Clark	1
B. Embleton	2
P. Schmidt	3
Records	4
WMC Ltd	5-7

This is copy No. 3 of 7.

1. EXPERIMENTAL METHODS

Six partially oriented specimens prepared from drill core samples of the Golden Mile Dolerite were supplied by Peter Williams. Specimens 294 and 295 contain primary magnetite and the remaining four specimens contain secondary magnetite.

Bulk susceptibilities were measured using a CSIRO balanced transformer bridge, which has a low operating frequency of 211 Hz. Natural remanent magnetisation (NRM) vectors were determined using a Digico flux gate spinner magnetometer and susceptibility anisotropy was measured on a Digico anistropy delineator.

2. SUSCEPTIBILITY AND REMANCENCE INTENSITY

The basic magnetic properties of the samples are given in Table 1. The susceptibilities are relatively high for basic igneous rocks of this age and correspond to average magnetite contents of ~1-2% by volume. There does not appear to be a pronounced difference in susceptibility between samples containing secondary magnetite and those containing primary magnetite. A significant difference in susceptibility of the two types of sample may exist, but much more extensive sampling would be required to characterise the properties adequately.

The NRM intensities of the specimens are quite variable and the magnitudes of the Koenigsberger ratios range from ~0.1 to ~1. It is noteworthy that, with the exception of sample 292, all NRM directions are closer to the down-hole direction than the up-hole direction i.e., broadly speaking, the NRM directions are "reversed" with respect to the present field direction. This fact is emphasised in the table by assigning negative signs to the NRM intensities and Q values of the reversely magnetised samples. Sample 292 suggests that both polarities of remanence may occur in the GMD sequence, but with only a single example of normal polarity, we cannot completely exclude the possibility that this sample was inadvertently inverted in the core tray or incorrectly marked up during preparation. Because the NRM of sample 292

is quite weak the polarity does not greatly affect the estimated average NRM intensity and Q value of the secondary magnetite bearing samples.

If the NRMs of GMD units are indeed of mixed polarity, the overall Koenigsberger ratio is less than that which would be obtained from the mean NRM intensity, calculated without regard to polarity. Scatter of NRM directions about the mean magnetisation direction further attenuates the effective Q value.

3. PALAEOMAGNETIC CLEANING

All specimens were subjected to alternating field (AF) demagnetisation in order to separate remanence components of different stability. This procedure is necessary to detect palaeomagnetic noise carried by magnetically soft grains, including effects due to exposure to stray magnetic fields, drilling or slicing. In many cases AF cleaning removes the palaeomagnetic noise, allowing determination of the remanence components which are representative of the bulk of the rock in situ.

The most effective way of presenting palaeomagnetic cleaning data is by Zijderveld plots, which are projections of end-points of successive remanence vectors onto a vertical plane (E-W or N-S) and onto the horizontal plane. Fig. 1 and the explanatory captions clarify the use of Zijderveld plots, using a hypothetical example of a two-component remanence.

Plots showing the response of the specimens to AF cleaning are given in Figs. 2-7. The directions are defined with respect to co-ordinate axes fixed in the specimen. Thus the indicated axes are not geographic. The open circles represent projection of vector end-points onto a "vertical" plane (containing the DDH axis) and the crosses represent projection onto the "horizontal" plane (i.e. the plane normal to the DDH axis). The "horizontal" axes N,E,S,W are arbitrary because of the initially unknown azimuthal orientation of the specimens. Note that when the samples were received it was assumed that the arrow marked on the sides indicated the down-hole direction rather than the up-hole

direction. Thus "UP" and "D" should be interchanged before comparing the apparent inclinations obtained from the plots with those given in Table 1. It was not possible to generate new plots with the correct sense for the "vertical" axes because of a breakdown of the Tektronix 4051 computer which produces these plots.

Monocomponent remanence is characterised by Zijderveld plots where both projections exhibit linear segments heading directly towards the origin. This behaviour simply reflects a gradual loss of remanence intensity with treatment in successively higher fields whilst the remanence direction remains unchanged. Palaeomagnetic noise is indicated by large, often erratic, changes in direction and intensity during the first few demagnetisation steps. Multicomponent magnetisations reflecting acquisition of remanence at more than one time in the geological history of the rock are revealed by multiple linear segments with distinct breaks in slope, provided the stability spectra of the components are discrete. If the components have partially overlapped stability spectra the linear segments are linked by curved segments. When the last few points on the plots do not trend towards the origin, there is a hard component present which has not been fully resolved (due to overlapped stability spectra or to swamping of the residual remanence by noise as the intensity drops to a small fraction of the NRM value).

Examination of Figs. 2-7 shows that the NRMs are not greatly perturbed by palaeomagnetic noise and are dominated by a single component, although in some specimens there is evidence of small unresolved hard components, that may have some geological significance, which could possibly be unravelled by a detailed palaeomagnetic investigation. The presence or absence of residual unresolved components is most clearly indicated by the insets in the Figures, which represent exploded views of the region around the origin. Specimens 291 and 296 are magnetically hard, with median destructive fields of 20 and 25 mT respectively. The other specimens are much softer, with mdfs in the range 2.5-6 mT. The palaeomagnetic signal of specimens 291 and 296 persists to fields greater than 100 mT indicating that is carried by fine single domain grains (possibly haematite as well as magnetite) in

addition to multidomain grains. The behaviour of the other specimens indicates that the remanence is carried by coarse multidomain magnetite.

Fig. 2 shows that AF cleaning of specimen 291 removes a shallow component, that is probably noise, revealing a steeper underlying component which has an inclination more consistent with those of other specimens. Cleaning of specimen 292 (Fig. 3) removes a small amount of noise, revealing a steep component which dominates the total magnetisation and is consistently removed in fields from 2 mT to 10 mT, before the residual remanence becomes affected by noise. The NRM of specimen 293 is dominated by a single steep component (Fig. 4), with no detectable noise component. Examination of the inset reveals that there is a very small unresolved component remaining after AF treatment to 25 mT.

The NRM of specimen 294 (Fig. 5) appears to be effectively monocomponent, with no evidence of noise or a residual hard component. The NRM of specimen 295 is dominated by a component with similarly steep inclination, but does also contain noise and hard components which are only, however, a small fraction of the NRM (Fig. 6).

Specimen 296 has a somewhat noisy plot (Fig. 7), but the end-points generally demagnetise towards the origin, indicating an essentially single component remanence.

The palaeomagnetic cleaning data demonstrate that the measured NRM vectors are not greatly affected by palaeomagnetic noise and are therefore representative of in situ remanence. Furthermore, the fact that the NRMs are dominated by a single component, subparallel to the down-hole direction, suggests that the overall remanence of the Golden Mile Dolerite in this area is relatively simple and that the remanence direction for this unit could be determined accurately with a relatively small collection of oriented samples.

4. NRM DIRECTIONS

The remanent intensities and Koenigsberger ratios of different samples cannot be combined vectorially because the samples are only

partially oriented. Aproximate intensities and Q values were calculated initially by projecting vectors onto the DDH axis and assuming the small orthogonal components are randomly distributed and tend to cancel each other. The approximation is quite good because the stronger remanences are subparallel to the DDH axis.

Because the samples are azimuthally unoriented it is not possible to obtain a unique estimate for the NRM direction. However the inclinations of the NRMs with respect to the DDH axis (azimuth 60°, dip 37.5° in the vicinity of the samples) are relatively steep. All relative inclinations are, in fact, greater than 30° (after conversion to consistent polarity), whereas there is a 50% probability for directions from a population which is uniformly distributed over a hemisphere to have inclinations less than 30°. Furthermore, 4 out of 6 samples have relative inclinations greater than or equal to 68°, i.e. they are crowded into a small spherical cap on the unit sphere, centred on the DDH axis, which only corresponds to 7% of the area of a hemisphere. This suggests that the NRM directions are not highly scattered, but systematically cluster in the NE down octant, subparallel to the DDH axis (or the SW up octant for "normal" directions).

5. MAGNETIC FABRIC AND ORIENTATION OF THE SAMPLES

The susceptibility anisotropy data are summarised in Table 2. These samples have anisotropy ratios which are higher than usual for basic igneous rocks, suggesting that the magnetic fabric is deformational. This supposition is supported by the pronounced magnetic lineation in most samples, which reflects alignment of the long axes of magnetite grains. The presence of this lineation is reflected in the triaxial nature of the susceptibility ellipsoids (i.e. there are significant differences between the major, intermediate and minor susceptibilities). Half the samples have predominantly prolate ellipsoids ($P > 1$), indicating that lineation is dominant. A pronounced magnetic lineation such as this usually indicates the direction of maximum extension (the major axis of the finite strain ellipsoid). Although the magnetic fabric is very clearly defined, the susceptibility anisotropy is not sufficiently large to significantly affect the induced magnetisation and the form of anomalies.

The magnetic foliation (plane of high susceptibility, containing the major and intermediate axes) in deformed rocks is normally parallel to the schistosity or cleavage. Where two intersecting schistosities of comparable strength are present, the magnetic foliation lies between the two schistosity planes and a magnetic lineation is generated along their line of intersection.

The minor susceptibility (k_3) axis is orthogonal to the major and intermediate axes, i.e. it represents the magnetic foliation pole. In Table 2 it is noteworthy that the inclinations of minor susceptibility axes, with respect to the DDH axis, are very consistent from sample to sample. This suggests that the magnetic foliation has a consistent orientation throughout the sampled zone, intersecting the DDH axis at an angle of ~65°, presumably parallel to the dominant cleavage. Assuming this to be so, we can use the magnetic fabric data to reduce the NRM vectors to a common azimuthal orientation, by rotating the fiducial marks on the specimens until the declinations of the k_3 axes are all coincident. The result yields a reasonably well-grouped set of NRM vectors (corrected to an arbitary common azimuthal orientation) which can be combined vectorially to yield an estimated mean direction for the GMD formation and a total remanence vector for the six samples.

Although this procedure corrects for the relative azimuthal orientations of the samples, the absolute orientation is uncertain unless the in situ attitude of the magnetic foliation can be determined. The cleavage in these rocks strikes towards 340° and dips ~70°W. Assuming the k_3 axes are parallel to the cleavage pole, and knowing that they lie 25° from the DDH axis, a direction for the magnetic foliation pole can be estimated. In fact, the estimated cleavage pole does not lie exactly on the cone of possible directions about the DDH axis. If the dip of the cleavage is assumed to be 76°, however, the cleavage pole does lie on the cone of half-angle 25° about the DDH axis, at the point (dec = 70°, inc = +24°). It is also possible to vary the strike of the cleavage, assuming the dip to be 70°, and obtain alternative solutions for the magnetic foliation pole at (40°, +20°) and (80°, +20°), corresponding to strikes of 310° and 350° respectively. It seems likely, however, that the strike of the cleavage

is more consistent and better known than the dip, which can probably vary somewhat. Therefore the preferred estimate of the k_3 axis is (70°, + 24°).

This estimate of the foliation pole provides the information required to orient the samples absolutely. When this is done the estimated NRM direction calculated irrespective of polarity, is dec = 28°, inc = +48° (N = 6, R = 5.67, K = 15.0) with a 95% cone of confidence (α_{95}) equal to 18°. This represents an estimate of the mean direction of in situ NRMs, independent of intensity. The vector sum of the NRMs, weighted according to intensity, is somewhat different because in this group of samples the more intense NRMs lie closer to the DDH axis. The vector mean NRM of all six samples is estimated to be Int = 1620 mA/m, dec = 45°, inc = +42° which, given the large error, is not significantly different from the above mean direction, derived from unit vectors.

Given the essentially monocomponent nature of the NRM, it is unlikely that there is a strong correlation between intensity and direction as the directions should be clustered about the palaeofield direction pertaining to the time of remanence acquisition, while the intensity depends mainly on magnetite content and grain size. Thus the difference between intensity-weighted and unweighted mean directions probably reflects a statistical fluctuation that is due to the small sample size. The best estimate of the average NRM direction is therefore that calculated from unit vectors, i.e. (28°, +48°), which is highly oblique to the present field. The mean AF cleaned direction is very similar and the remanence is clearly very ancient. Since primary remanence is usually heavily overprinted by greenschist facies or higher grade metamorphism, this remanence component probably represents a metamorphic overprint.

The procedure described above for finding the orientation of the remanance can also be applied to the susceptibility axes of the individual specimens. Once the axes of individual specimens are reduced to a common azimuthal orientation the susceptibility ellipsoids can be combined tensorially to calculate a mean susceptibility ellipsoid. The

magnetic fabric parameters for all six specimen combined are found to be A = 1.19, L = 1.11, F = 1.07, P = 1.04, $\overline{k}$ = 0.0556. The minor axis is (70°, + 24°), by hypothesis, and the major axis corresponds to the projection of the mineral lineation onto the magnetic foliation plane, i.e. (166°, + 25°). The intermediate axis is orthogonal to the other two, by definition. This procedure was carried out for the primary magnetite bearing specimens and secondary magnetite bearing specimens as well. The induced magnetisations calculated from the susceptibility ellipsoids are given in Table 3, together with the orientation-corrected remanence vectors and the resultant magnetisations.

6. IMPLICATIONS FOR MODELLING

The results listed in Table 3 essentially confirm the approximate estimates of Koenigsberger ratios given in Table 1. The Q values for the primary magnetite bearing samples and secondary magnetite bearing samples are, respectively, 0.81 and 0.44. For all samples combined Q = 0.57. The results suggest that, although remanence does not dominate the total magnetisation, it is nevertheless important and should be considered in modelling. The overall effect of the remanence is to deflect the resultant magnetisation vector toward the east and toward the horizontal, without greatly affecting the magnetisation intensity. The resultant intensity is in fact about 5-10% lower than the induced intensity and the angle of deflection from the present field direction is 45° for the primary magnetite bearing samples, 22° for the secondary magnetite bearing samples and 30° for all samples.

The induced magnetisations are not exactly parallel to the Earth's field because of the anisotropy. The deflections of the induced magnetisation vectors are only about 7°, and the effect of anisotropy can be safely neglected in most modelling applications.

7. CONCLUSIONS

(i) No clearly defined difference between the magnetic properties of primary magnetite bearing and secondary magnetite bearing samples was found. This may simply reflect the limited sampling.

(ii) Remanence makes a substantial, although not dominant, contribution to the total magnetisation of the GMD samples. The remanence direction is estimated as (28°, + 48°), with a 95% cone of confidence equal to 18°. The effective Koenigsberger ratio is ~0.6. Both polarities of remanence may be present in the GMD. The resultant magnetisation (induced plus remanent) is shallower and more easterly than the present field direction. Quantitative modelling should therefore take remanence into account.

(iii) AF cleaning demonstrates that the NRMs are dominated by a single ancient component, with negligible palaeomagnetic noise. The measured NRMs and the calculated Q values are therefore representative of the in situ values for these samples. The NRM directions appear to be well-grouped.

(iv) Based on AF cleaning data, samples 291 and 296 contain fine single domain grains of magnetite (which are submicroscopic) or haematite, as well as multidomain magnetite grains. The other samples are relatively soft and contain large multidomain (>100 μm) grains.

(v) All samples exhibit a clearly defined magnetic fabric with a foliation (plane of higher susceptibility) containing a lineation (direction of maximum susceptibility). The anisotropy degree and the prolateness of the susceptibility ellipsoids are atypically high for dolerites and suggest that the magnetic fabric is deformational. The orientation and strength of the magnetic fabric elements appears to be similar for samples containing primary or secondary magnetite, implying that the fabric results from re-orientation of pre-existing magnetite grains. This suggests that the deformation is younger than the secondary magnetite. In deformed rocks the magnetic foliation is nearly always parallel to the cleavage or schistosity. Assuming this to be so for the GMD allows the azimuthal orientation of the specimens to be determined.

TABLE 1 MAGNETISATION OF GOLDEN MILE DOLERITE SAMPLES

Sample	k_z(SI)	J_n(mA/m)	Q	I'_n	Polarity	Magnetite
291	0.0336	-245	-0.16	+35°	R	S
292	0.0266	+215	+0.17	-74°	N	S
293	0.1262	-4800	-0.82	+80°	R	S
294	0.0571	-3040	-1.15	+78°	R	P
295	0.0545	-1990	-0.79	+68°	R	P
296	0.0116	-42	-0.08	+42°	R	S
Primary magnetite combined	0.0558	~-2515	~-1.0		R	P
Secondary magnetite combined	0.0495	~-1200	~-0.5		R	S

k_z = bulk susceptibility measured along DDH axis ($k_{cgs} = k_{SI}/4\pi$)

J_n = NRM intensity (1mA/m = 1μG)

Q = Koenigsberger ratio = J_n/kH (H = 46,155 mA/m)

I'_n = inclination of NRM with respect to DDH axis (positive downwards)

Polarity : N = "normal", R = "reversed" with respect to present field direction

TABLE 2 SUSCEPTIBILITY ANISOTROPY OF GMD SAMPLES

Sample	$\overline{k}$ (SI)	A	L	F	P	I_3'
291	0.0348	1.11	1.01	1.10	0.92	60°
292	0.0275	1.10	1.05	1.05	1.00	61°
293	0.1395	1.27	1.21	1.05	1.15	71°
294	0.0628	1.22	1.10	1.11	1.00	77°
295	0.0548	1.19	1.09	1.08	1.01	61°
296	0.0123	1.20	1.13	1.06	1.06	62°

$\overline{k}$ = bulk susceptibility = $(k_1 + k_2 + k_3)/3$

k_1 = major susceptibility, k_2 = intermediate susceptibility, k_3 = minor susceptibility ($k_1 > k_2 > k_3$)

A = anisotropy ratio = k_1/k_3

L = magnetic lineation strength = k_1/k_2

F = magnetic foliation strength = k_2/k_3

P = prolateness of susceptibility ellipsoid = L/F

I_3' = inclination of minor susceptibility axis, with respect to DDH axis.

TABLE 3 ORIENTATION-CORRECTED MAGNETISATIONS

	NRM	Induced	Resultant	Q
Primary magnetite	2500;48°,+46°	3090;344°,-65°	2780;21°-21°	0.81
Secondary magnetite	1200;45°,+35°	2710;343°,-64°	2560;10°,-43°	0.44
All	1620;45°,+42°	2830;343°,-64°	2560;14°,-35°	0.57

Magnetisations expressed as : Intensity (mA/m); Declination, Inclination

Magnetisation is a three dimensional vector quantity and difficulties arise when representing such on a flat surface. Two separate figures are required to display a three dimensional vector. Stereographic plots and an intensity decay curve have been very useful, especially when the direction of the cleaned magnetisation is of paramount importance. However, when an appreciation of the full vectorial nature of a magnetisation is required, orthogonal projections (Zijderveld, 1967) provide an ideal method of combining both the magnitude and directional information. This greatly assists the recognition and identification of multi-component magnetisations.

(a) This illustration portrays the magnetisation decay during eight demagnetisation steps, from an oblique perspective (southeast-up octant). $\tilde{J}_1 - \tilde{J}_2$ represents the vector difference between the first and second demagnetisation step, i.e. the magnetisation removed during the second step.

(b) By simply plotting the vector end-points the diagram is greatly clarified and a soft $(\tilde{J}_s)$ and hard $(\tilde{J}_h)$ magnetisation are evident, yet a unique identification of the direction or intensity of either is not possible from this single figure.

(c) Linear combination of magnetisations yields a resultant NRM $(\tilde{J}_o)$.

(d) By projecting vector end-points onto the horizontal plane and a vertical plane allows the composition of the magnetisation to be visualised.

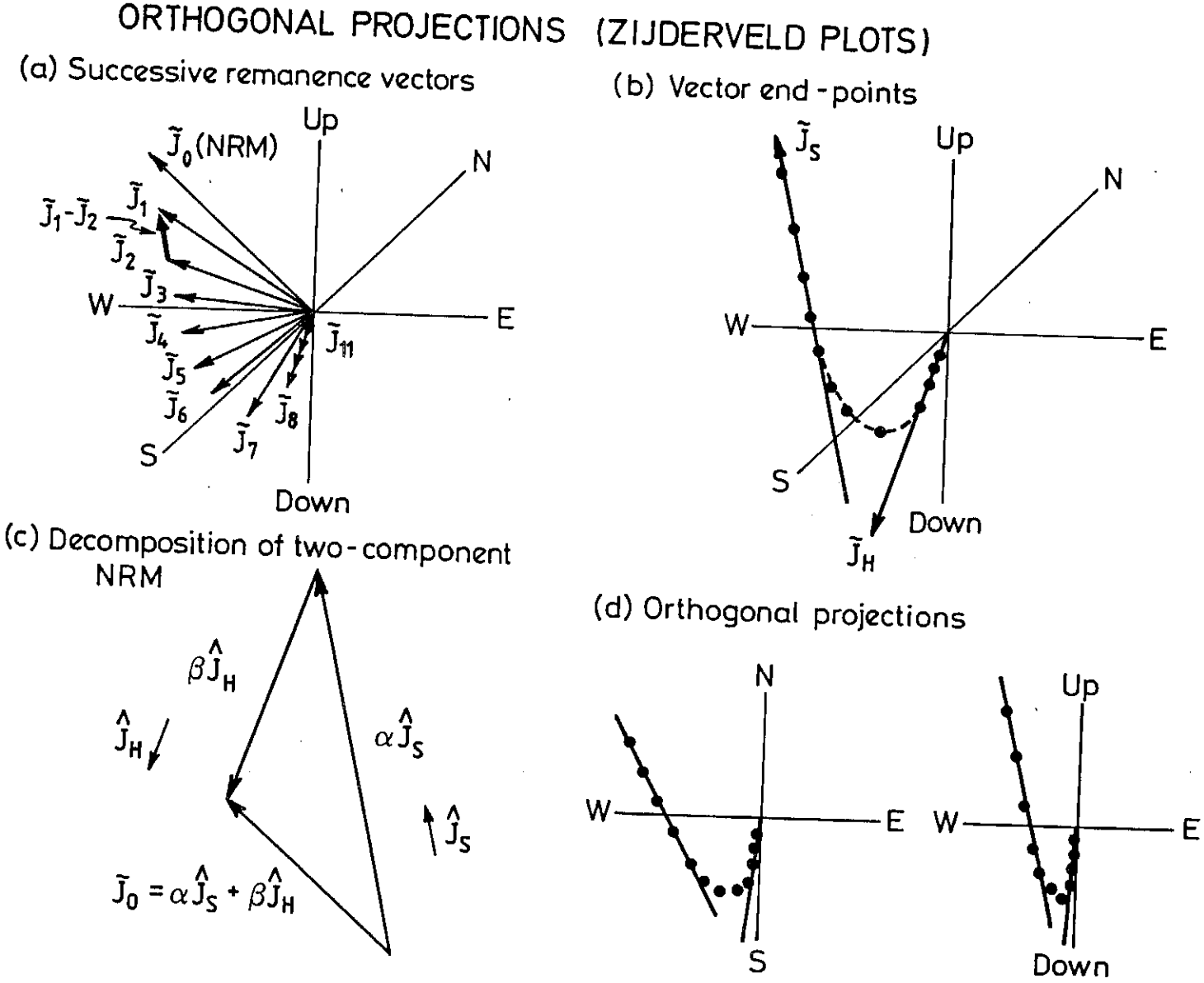
ORTHOGONAL PROJECTIONS (ZIJDERVELD PLOTS)
(a) Successive remanence vectors
$\tilde{J}_0$(NRM)
$\tilde{J}_1$-$\tilde{J}_2$
$\tilde{J}_1$
$\tilde{J}_2$
$\tilde{J}_3$
$\tilde{J}_4$
$\tilde{J}_5$
$\tilde{J}_6$
$\tilde{J}_7$
$\tilde{J}_8$
$\tilde{J}_{11}$
Up
N
E
W
S
Down
(b) Vector end-points
$\tilde{J}_S$
$\tilde{J}_H$
Up
N
E
W
S
Down
(c) Decomposition of two-component NRM
$\beta\hat{J}_H$
$\hat{J}_H$
$\alpha\hat{J}_S$
$\hat{J}_S$
$\tilde{J}_0 = \alpha\hat{J}_S + \beta\hat{J}_H$
(d) Orthogonal projections
N
W
E
S
Up
W
E
Down

FIG. 1A

When two components of magnetisation are present with overlapping stability spectra there is a range of treatment steps for which both components are removed.

(a) If two components are removed at the same rate they will be projected as straight lines resulting in the identification of a false, or spurious, components.

(b) Stereoplots of the measured vectors and the vector difference directions of the same components plotted in (a).

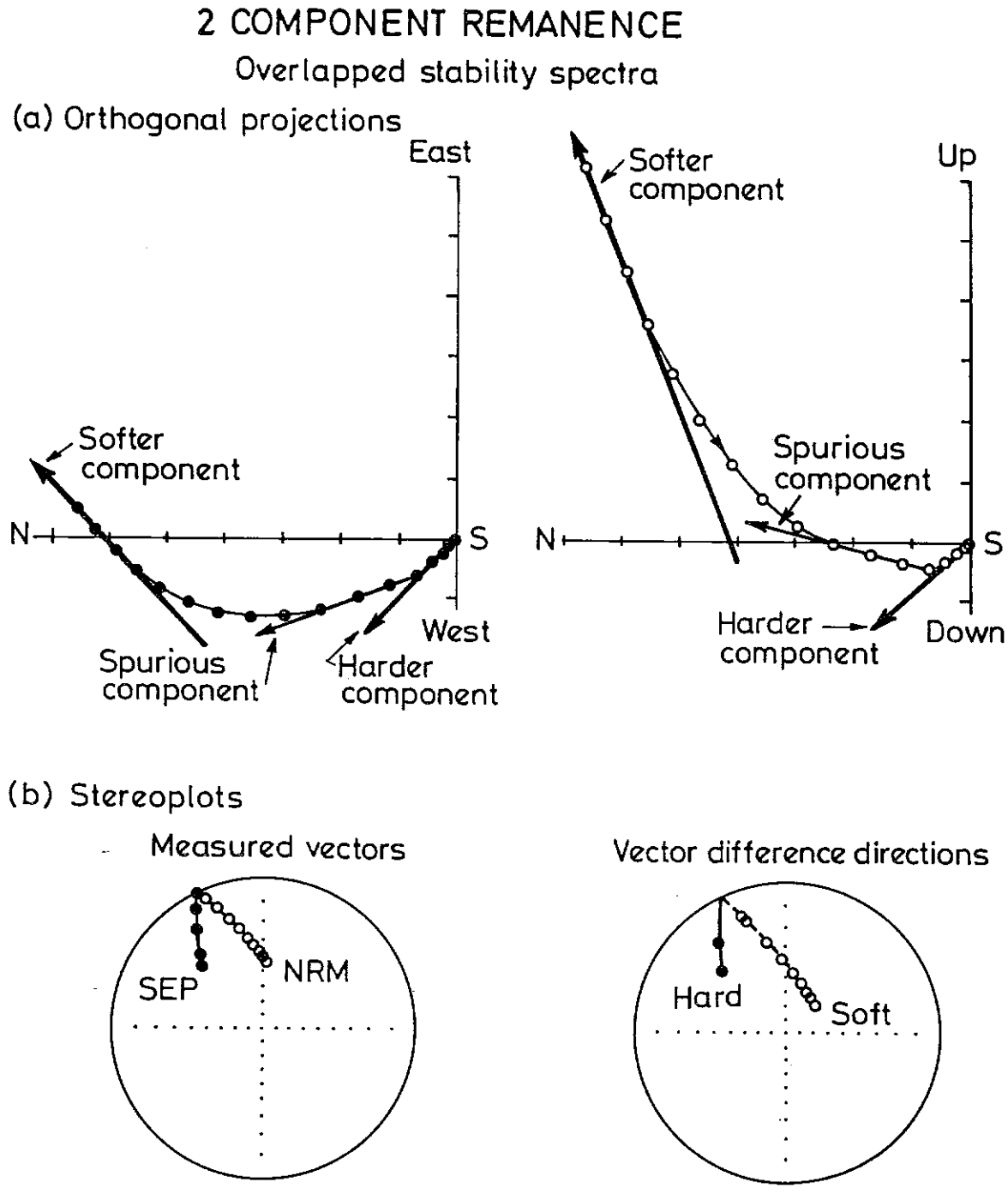
2 COMPONENT REMANENCE
Overlapped stability spectra
(a) Orthogonal projections
East
Softer component
N
S
West
Spurious component
Harder component
Up
Softer component
Spurious component
N
S
Harder component
Down
(b) Stereoplots
Measured vectors
SEP
NRM
Vector difference directions
Hard
Soft

FIG. 1B

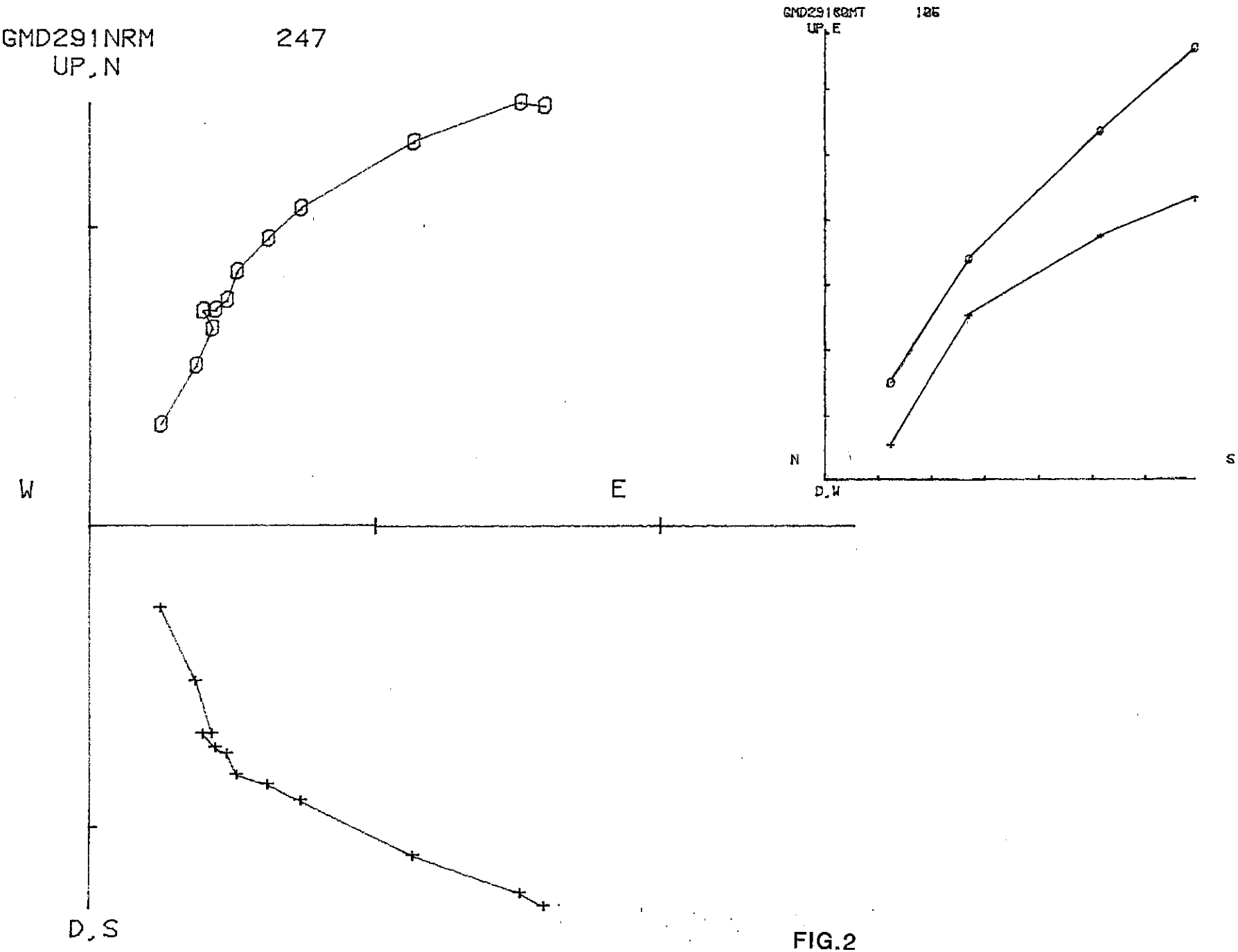

FIG.2

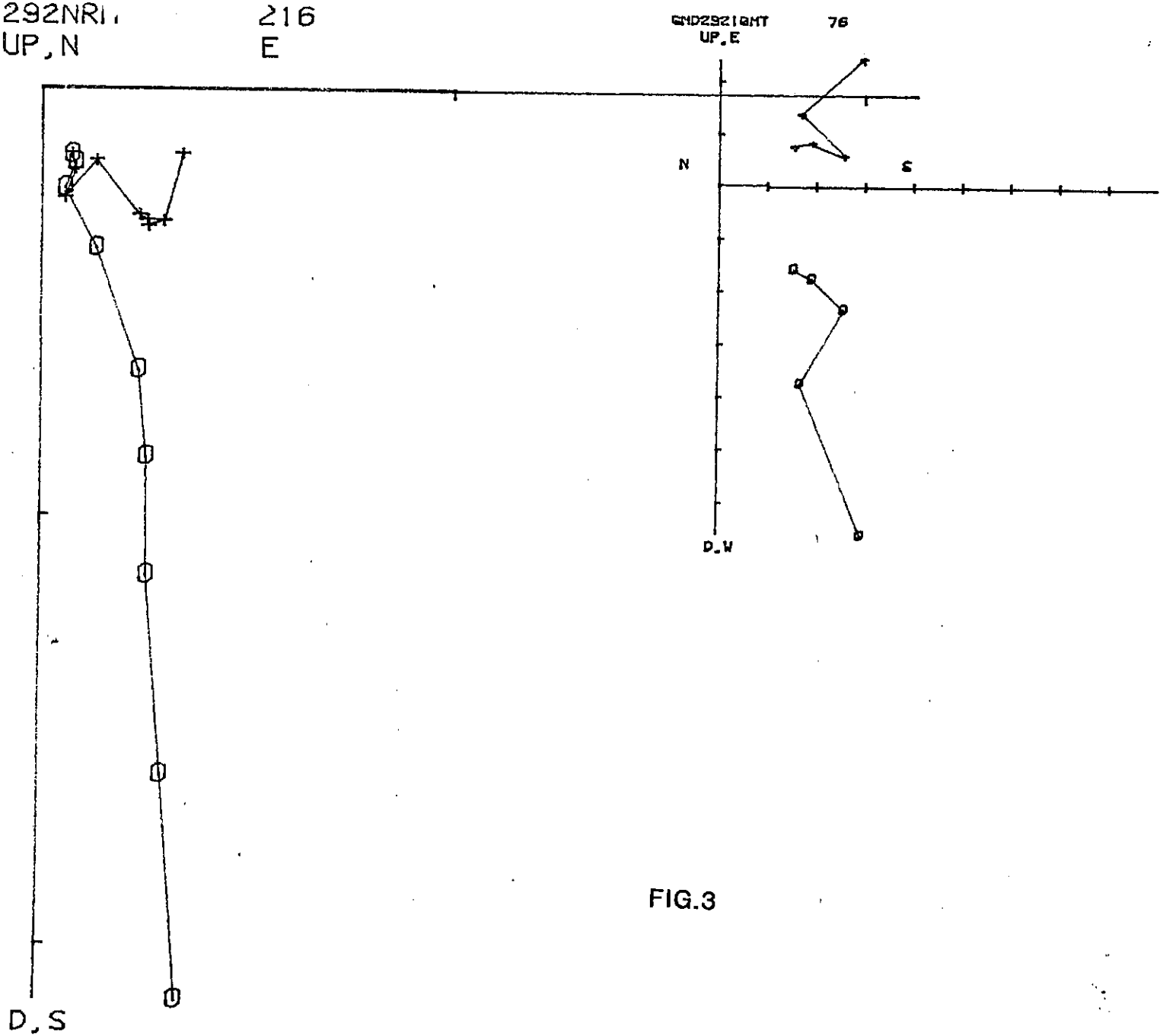

FIG.3

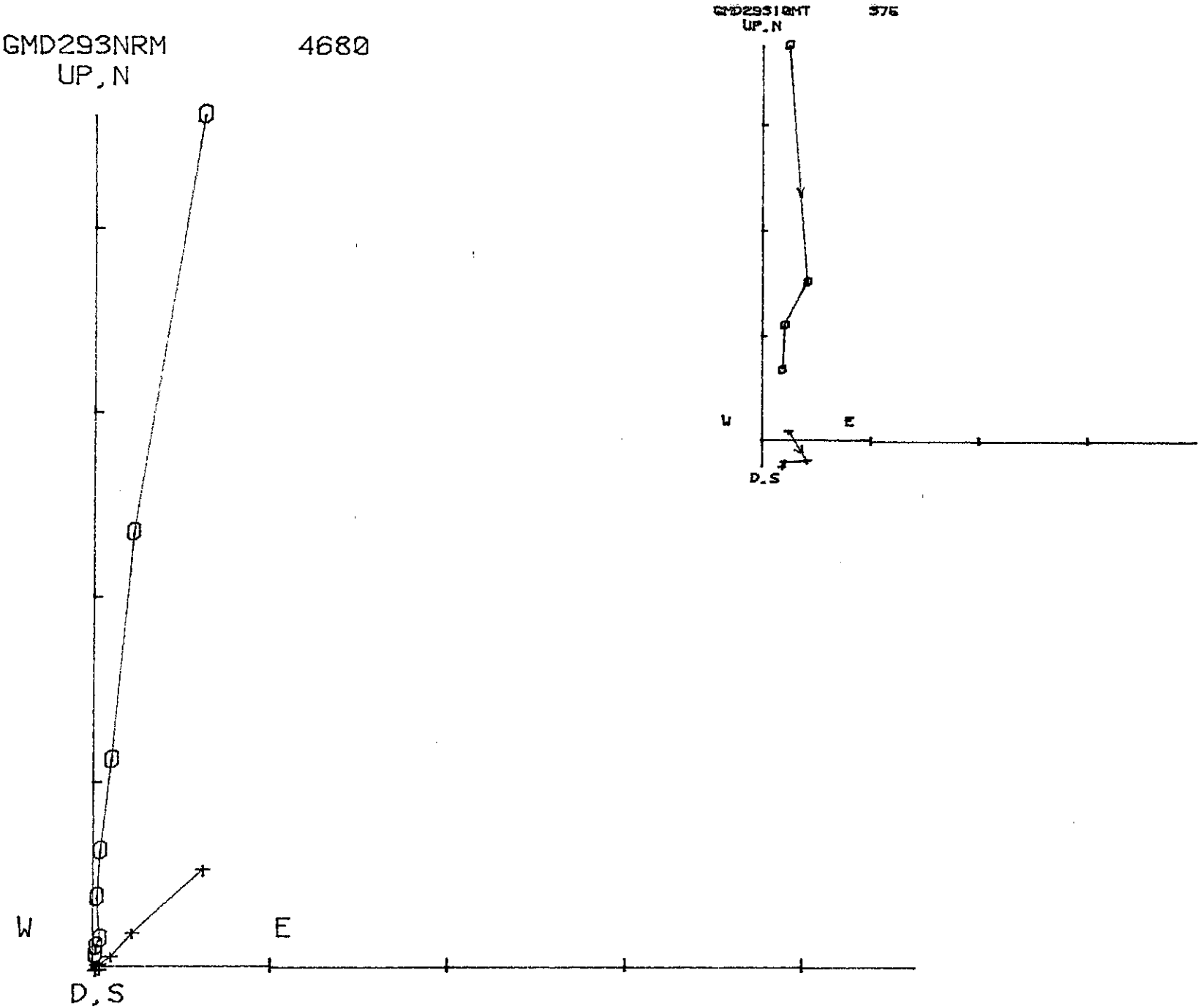

FIG.4

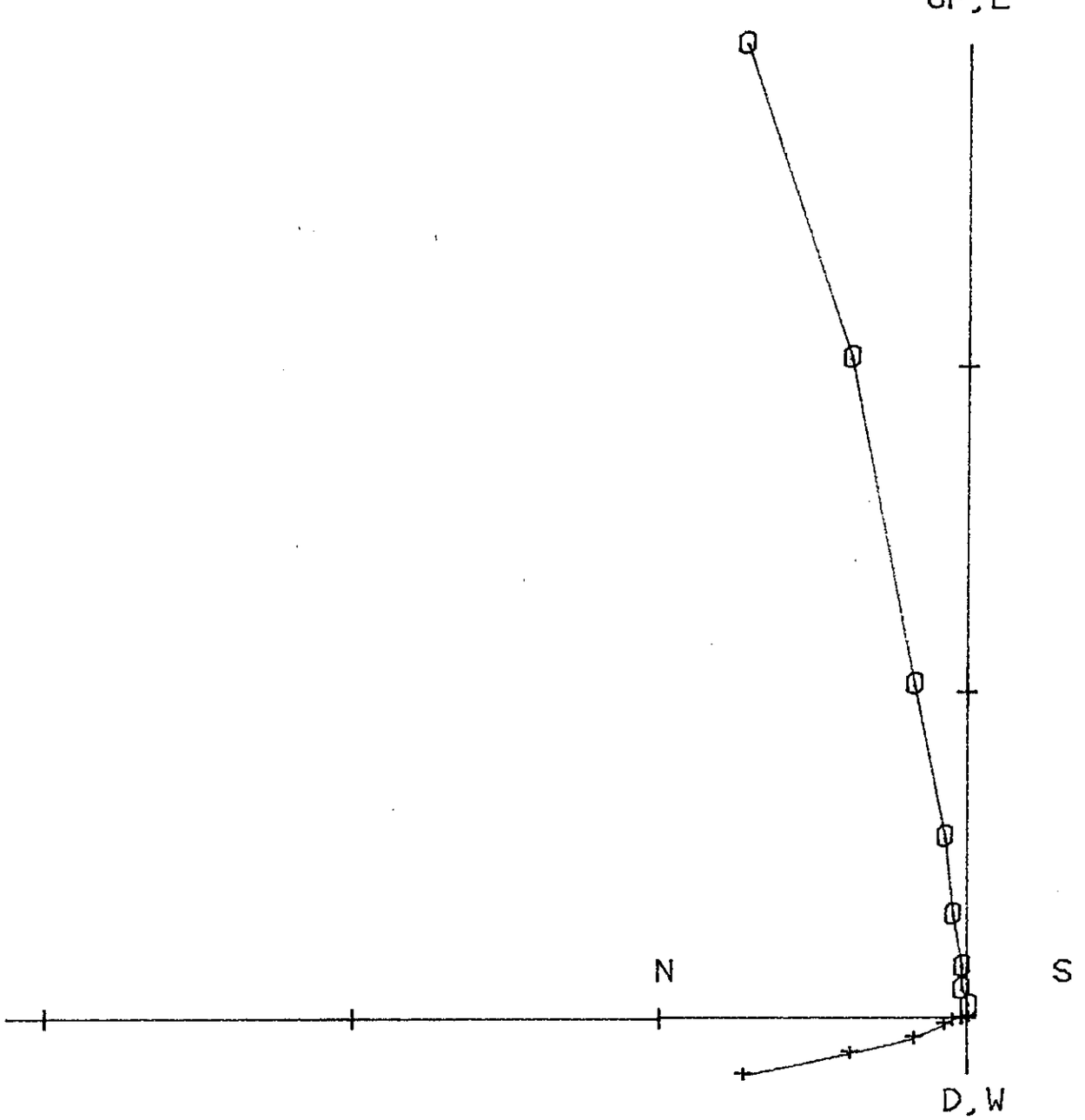

FIG.5

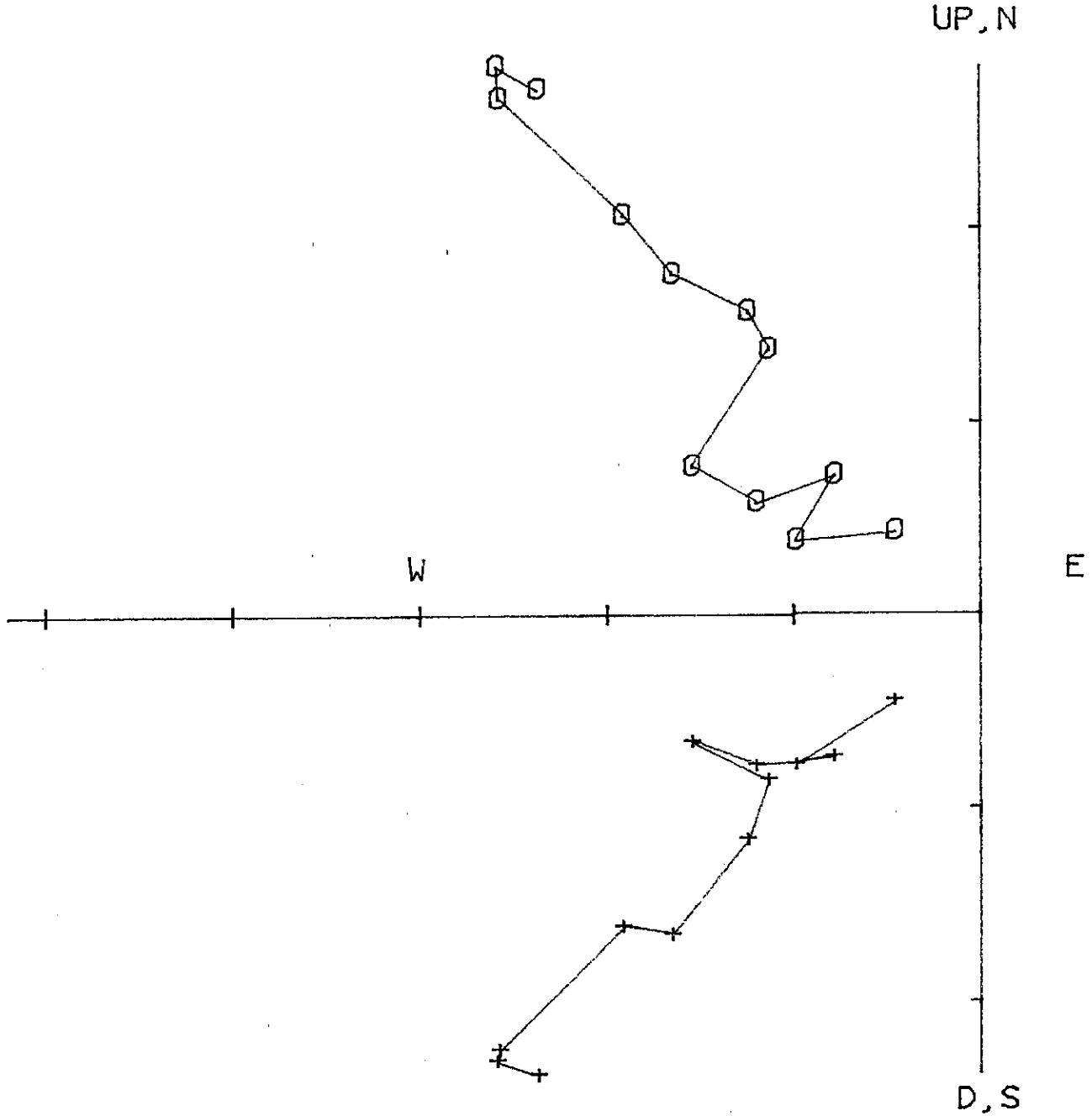

FIG.7